

OSIRIS-REX ORBIT DETERMINATION COVARIANCE STUDIES AT BENNU

P.G. Antreasian,^{*} M. Moreau,[†] C. Jackman,^{*} K. Williams,^{*} B. Page,^{*}
and J.M. Leonard^{*}

The Origins Spectral Interpretation Resource Identification Security Regolith Explorer (OSIRIS-REx) mission is a NASA New Frontiers mission launching in 2016 to rendezvous with the small, Earth-crossing asteroid (101955) Bennu in late 2018, ultimately returning a sample of regolith to Earth. Approximately three months before the encounter with Bennu, the asteroid becomes detectable in the narrow field PolyCam imager. The spacecraft's rendezvous with Bennu begins with a series of four Asteroid Approach Maneuvers, slowing the spacecraft's speed relative to Bennu beginning two and a half months prior to closest approach, ultimately delivering the spacecraft to a point 18 km from Bennu in Nov, 2018. An extensive campaign of proximity operations activities to characterize the properties of Bennu and select a suitable sample site will follow. This paper will discuss the challenges of navigating near a small 500-m diameter asteroid. The navigation at close proximity is dependent on the accurate mathematical model or digital terrain map of the asteroid's shape. Predictions of the spacecraft state are very sensitive to spacecraft small forces, solar radiation pressure, and mis-modeling of Bennu's gravity field. Uncertainties in the physical parameters of the central body Bennu create additional challenges. The navigation errors are discussed and their impact on science planning will be presented.

INTRODUCTION

In the fall of 2018, NASA's OSIRIS-REx (OREx) spacecraft (S/C) will encounter the small Earth-crossing B-type asteroid, Bennu, with the objective to acquire a sample of the asteroid's regolith and return it to Earth. Activities onboard the S/C will increase 3 months before the encounter when the asteroid finally becomes detectable in the narrow field PolyCam imager. The S/C's rendezvous with Bennu, which is independent of launch date, begins with a series of four Asteroid Approach Maneuvers (AAMs), which slow the S/C's speed relative to Bennu beginning two and one half months prior to closest approach of 18 km on November 18, 2018. During this time, navigation is dependent on star-based Optical Navigation (OpNav) images of the asteroid and 2-way X-band Doppler and range via the Deep Space Network (DSN). During the approach to Bennu, several observations will be devoted to searching for satellites in orbit about the asteroid. If none are found, the mission will proceed with the Navigation Campaign, which will allow the Navigation Team approximately two months to determine the dynamical environment at close proximity to Bennu accurately enough to achieve the Science objectives in subsequent phases and ultimately acquire a sample during the Touch And Go (TAG) event.

^{*} KinetX, Inc., Space Navigation and Flight Dynamics Practice, 21 W. Easy St., Ste 108, Simi Valley, CA 93065 USA.

[†] NASA/GSFC Code595, 8800 Greenbelt Rd, Greenbelt, MD 20771, USA.

ORBIT DETERMINATION PROCESS

Orbit Determination (OD) is the process of estimating the S/C's state (position and velocity) by minimizing in a least squares sense the residuals of tracking data observables and computed observables. The computed observables are based on a dynamical model of the S/C's equations of motion due to gravity, SRP, S/C maneuvers and momentum desaturation events (desats), and other small non-gravitational forces.

During flight operations, OD is geared towards the generation and delivery of certain data products used by the project. The types of products produced by the OD team throughout the mission are given below:

- **Maneuver Designs:** Prior to a planned maneuver, an estimated trajectory and its uncertainty is predicted forward to the maneuver epoch in order to design the maneuver.
- **Knowledge Updates:** Prior to a planned mission phase, an estimated trajectory and its uncertainty is predicted forward for use in generating or updating the sequence aboard the S/C.
- **Trajectory Reconstructions:** At specific times, the data arc is terminated and used to provide an improved estimate of the trajectory and associated uncertainties at points interior to the data arc to assist in science data reduction.
- **Maneuver Reconstructions:** Data before and after a TCM are used to estimate maneuver parameters with the objective to improve their future designs.
- **Tracking Prediction Updates:** Trajectory updates given to the DSN for antenna pointing predictions and for proper up-link and down-link tracking of radio frequencies.

ProxOps Filter Strategy

Computation and prediction of the S/C's trajectory is accomplished by numerical integration of the equations of motion using the MIRAGE software. The integrated S/C ephemeris and other trajectory-related products are used throughout the mission to support maneuver design and analysis, S/C engineering analysis, sequence development, mission planning, and DSN operations.

In general terms, the dynamics of the trajectory are modeled by a set of nonlinear ordinary differential equations. The acceleration of the S/C in the inertial frame can be represented by

$$\ddot{\vec{r}} = \ddot{\vec{r}}_g + \ddot{\vec{r}}_{SRP} + \ddot{\vec{r}}_{NGA} \quad (1)$$

where $\ddot{\vec{r}}_g$ is the S/C acceleration due to gravitational forces, $\ddot{\vec{r}}_{SRP}$ is the S/C acceleration due to SRP and $\ddot{\vec{r}}_{NGA}$ is the S/C acceleration due to other small non-gravitational forces caused by factors such as desats, albedo and infrared radiation pressure from the asteroid, thermal re-radiation of the S/C and outgassing. Figure 2 shows the major forces acting upon the S/C during proximity operations at Bennu.

For the Bennu proximity operations phase, the gravitational forces of Bennu due to oblateness are modeled by a 15x15 spherical harmonic representation. Initially, this model is derived from a shape model that assumes a constant density. However, throughout ProxOps, the non-spherical gravity model of Bennu will be updated with current best estimates. Note at the 1-km orbit, the trajectory is not sensitive to terms higher than degree and order 4.

A box-wing plate model of the S/C has been developed and implemented in MIRAGE for use with SRP modeling and non-gravitational accelerations such as asteroid albedo and infrared radiation pressure. This shape model of the S/C uses 10 flat plates representing a 6-sided Bus and the front and backs of the two solar panels. The 10-plate model consists of areas and optical

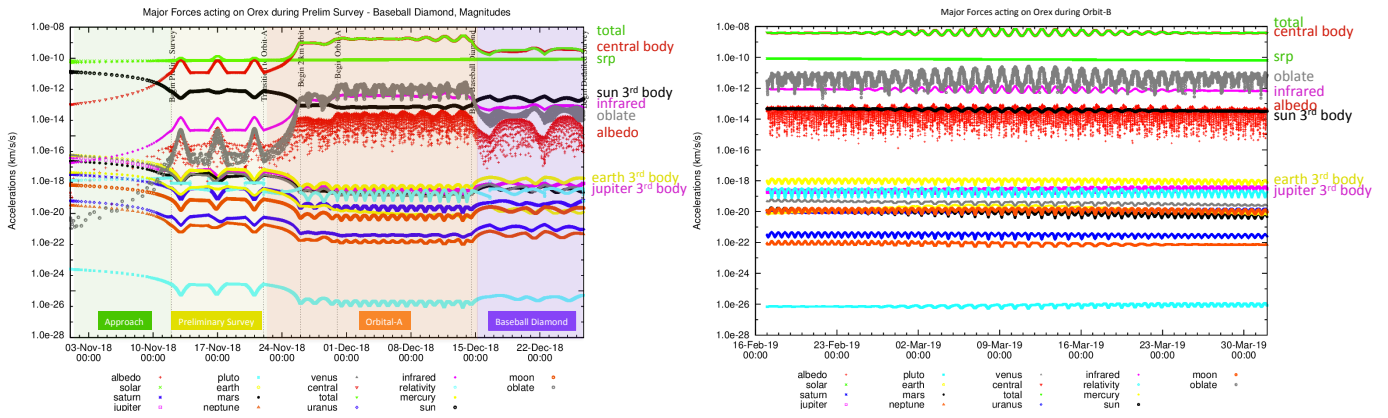


Figure 2: Major forces acting on OREx during early ProxOps (left) and Orbital-B (right)

properties (specular and diffuse coefficients) derived from the S/C properties provided by Lockheed Martin (LM) [Olds, 2013]. The SRP magnitude ranges from 65 nm/s² at perihelion in January 2019 to 28 nm/s² at aphelion in September of 2019.

The acceleration due to small non-gravitational forces can be expressed as

$$\ddot{\vec{r}}_{\text{NGA}} = a_R \hat{u}_R + a_X \hat{u}_X + a_Y \hat{u}_Y \quad (2)$$

where a_R , a_X , and a_Y represent acceleration magnitudes in the corresponding unit directions. The unit vectors \hat{u}_R , \hat{u}_X , and \hat{u}_Y are defined in a spacecraft local coordinate system for which the directions are defined as follows: \hat{u}_R is in the anti-Sun direction, \hat{u}_Y is normal to the plane formed by \hat{u}_R and the spacecraft's nominal velocity vector, \vec{v}_{ref} , and \hat{u}_X completes the right-handed orthonormal triad.

These parameters are used to approximate small, S/C induced anomalous forces derived from thermal re-radiation, material out-gassing, gas leakage from valves and pressurized tanks, and other small effects. The significance of these accelerations lies in their effect on the OD process and uncertainty predictions. They are typically modeled as random processes due to the fact that the trajectory perturbations due to these phenomena are typically quite small and random in nature. The typical accelerations derived from these processes during ProxOps are assumed to range from 1 to 3 nm/s². However, trajectory perturbations at these levels can induce significant down-track errors when in close proximity to a small asteroid, especially when evaluating the impact on science observations two or more days after the OD data cut off (DCO). One of the major challenges will be to characterize these errors below the 3 nm/s² level to help with science planning. In addition, since the onboard S/C ephemeris is used to target nadir pointing OpNav images, it will be necessary to update the onboard ephemeris to keep Bennu within the NavCam image at least twice per week during the 1-km orbit, because down-track errors could grow over 100 m within 3–4 days.

Spacecraft Thermal Re-radiation Force

A model of the S/C thermal re-radiation has been developed to aid in the predictive accuracy of the trajectories delivered to the project for sequence and Science planning. The force (acceleration) upon the S/C in the S/C body-fixed frame resulting from the S/C's thermal (infrared) emissive radiation imbalance can be computed to first order as a function of time:

$$\begin{aligned}
\vec{a}_{S/CIR}(t) = & -\frac{2\sigma}{3mc} \left(\left[A_X(\epsilon_{+X}T_{+X}^4(t) - \epsilon_{-X}T_{-X}^4(t)) + A_{SA}(\epsilon_f T_f^4(t) - \epsilon_b T_b^4(t)) \cos \theta \right] \hat{x} \right. \\
& + A_Y(\epsilon_{+Y}T_{+Y}^4(t) - \epsilon_{-Y}T_{-Y}^4(t)) \hat{y} \\
& \left. + \left[A_Z(\epsilon_{+Z}T_{+Z}^4(t) - \epsilon_{-Z}T_{-Z}^4(t)) - A_{SA}(\epsilon_f T_f^4(t) - \epsilon_b T_b^4(t)) \sin \theta \right] \hat{z} \right)
\end{aligned} \tag{3}$$

where m is the S/C mass, c is the speed of light, σ is Stefan-Boltzmann constant, θ is the solar panel tilt angle, T_f is temperature on the front of the solar array, T_b is the temperature on the back of the solar array, and A_i , ϵ_i , and $T_i(t)$ are the projected area, area-averaged emissivity and area-averaged temperature, respectively, on each face of the bus or solar array. The S/C body coordinate frame is used. This assumes each face of the bus can be modeled as flat plates, which are normal to the body-fixed axes.

Research on this force (Ref. Sugimoto [2010], Shoemaker [2012], Antreasian [1992], Vique [1994], and Fahnstock [2012]) for vehicles in the 1 AU solar distance range generally show that the resultant force can be as much as 10% of the SRP affect. The above equation for the thermal force depends on the on-orbit temperatures of the S/C. The computation of the expected temperatures in close proximity to Bennu was performed by the Lockheed-Martin thermal engineer, C. May, using a full thermal-finite-element analysis of the S/C. The thermal model of the S/C contains over 6000 external nodes. Each node is represented by a projected area and optical properties (reflectivity, emissivity). Temperature histories were computed during the 1-km Orbital-B orbit assuming the nominal Z-to-nadir, X-to-Sun attitude (see Figure 3 (a)) and during a time that assumes a 5-hour High Gain Antenna (HGA)-to-Earth (X-to-Earth) pointing attitude. The solar arrays are rotated 45° about the +Y-axis for both attitudes. At each point in the orbit, the contribution of energy imbalances of each node are summed along each S/C body-fixed axes to determine the acceleration due to thermal re-radiation.

Two thermal models were received from Lockheed Martin: 1) the first model was evaluated during late Orbital-B at the time of TAG in October 2019 when Bennu is near aphelion at 1.3 AU; and 2) the second model was evaluated during early Orbital-B (March 2019) when Bennu just passes perihelion at 0.98 AU. The data included temperatures, emissivities and areas for each external node on each side of the S/C bus and solar arrays for four locations in the 1-km sun-terminator orbit. The locations include Bennu’s North Pole, South Pole, and equator crossings at sunrise and sunset for nominal attitude and one point for HGA-to-Earth point attitude when the Sun-probe-Earth (SPE) angle is $\sim 72.5^\circ$. Since model 1 was evaluated at Bennu’s aphelion when temperatures are generally lower, these numbers are considered to be near the lower bound of the expected thermal force during ProxOps. And because model 2 incorporated higher temperatures during perihelion, this model represents the expected upper bound to the S/C thermal force.

Figure 3 (a) illustrates the orbital positions and attitudes evaluated in model 2. Figure 3 (b) shows the thermal accelerations from model 2. These values are compared to model 1 in Table 1. The total X or Z-axis force includes the contribution of the solar array in the last columns. The forces during perihelion are roughly 2-3 times those during aphelion. The forces along the S/C X and Z-axes during the nadir-point attitude, which are in respectively, the sun (orbit normal) and radial directions are not expected to perturb the orbit’s down-track position. The force along the Y-axis, which is primarily in the orbit transverse direction during nadir-point attitude, is two orders of magnitude lower than the totals in the X or Z directions. If this level of imbalance proves to be accurate in operations, then the assumed down-track non-gravitational errors are conservative.

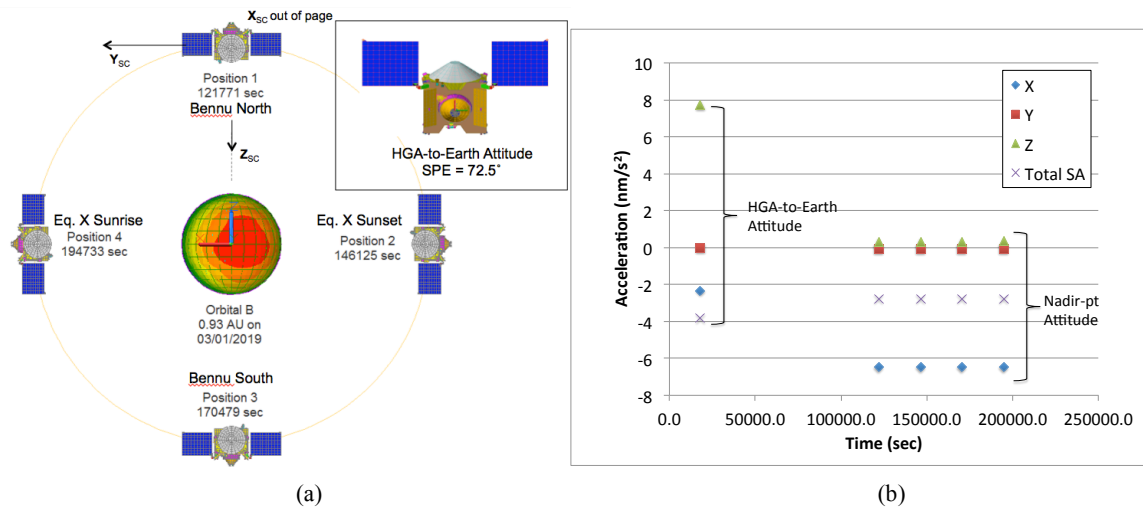


Figure 3: a) Orbital locations, attitudes evaluated for model 2. b) S/C thermal accelerations during Orbital-B March 2019

In operations, temperature telemetry will be available at various locations on the S/C bus. These bus temperatures, however, will be internal to outside blankets and therefore, further computations are needed to determine the temperatures on the outside blankets based on the thermal conductivity of the blankets. Further work will be performed by the thermal engineer to calibrate the full-up thermal model in operations.

Table 1: S/C Thermal accelerations along S/C body-fixed directions

Thermal Model	Solar Dist	Attitude	Along Each S/C Axis (Face only)				Total	
			X (nm/s ²)	Y (nm/s ²)	Z (nm/s ²)	Solar Arrays (nm/s ²)	+X + SA (nm/s ²)	+Z + SA (nm/s ²)
Model 1	1.35	Nadir	-2.58	-0.04	-0.02	-0.90	-3.22	-0.80
		HGA	-1.46	-0.03	2.63	-0.72	-1.97	2.12
Model 2	0.93	Nadir	-6.47	-0.05	0.31	-2.78	-8.44	-1.65
		HGA	-2.33	-0.03	7.71	-3.83	-5.04	5.00

The MIRAGE pseudo-epoch state batch processor will be used throughout the mission to process radiometric tracking and optical navigation observables to estimate the S/C's state. The baseline parameters that will always be estimated in the filter will include the S/C's state (position and velocity), maneuvers, desat events, SRP parameters, and small forces. The Benu ephemeris, GM and gravity harmonics up to degree and order 4 will also be estimated during proximity operations at Benu. Other parameters will be added throughout the mission as well as the uncertainties of other consider parameters. Appendix A lists the filter parameters estimated and considered for ProxOps as well as data weights and *a priori* uncertainties.

OpNav Tracking

OpNav imaging is a vital contributor to the OD during asteroid proximity operations. While DSN radiometric ranging and Doppler is necessary for OD throughout the duration of the mission, these data types provide limited information when orbiting unknown bodies due to uncertainties in their ephemeris and physical properties. Thus, it is necessary to supplement radiometric data with an observation that allows for direct characterization of the unknown body. Optical images provide such information and their use in navigation near small bodies like Benu is essential to ensure accurate orbit determination of the S/C during the course of proximity operations.

Two OpNav techniques will be employed throughout proximity operations at Bennu. The first method is a star-based OpNav method whose objective is to determine the position of the target body’s center through a series of images. This is a two-step process. First the camera pointing errors must be removed through imaging of the background stars and using their locations to solve for the pointing errors. Next, the target body is imaged resulting in a set of images that can be used to obtain the center of the target body. KXIMP is the primary star-based OpNav software used for OSIRIS-REx. KXIMP was developed by KinetX and was used successfully on the New Horizons mission to Pluto. This software will be used extensively from Approach through Orbital-A [Jackman, et al., 2016].

Star-based OpNav will treat Bennu as an unresolved object until its diameter exceeds a few pixels. The center of Bennu will be estimated by cross-correlating the observed image with a Gaussian Point Spread Function model. When the diameter exceeds a few pixels, star-based OpNav will transition to treating Bennu as an extended body. The center will be estimated by cross-correlating the observed image against the *a priori* shape model of the body, thus providing improved information on the ephemeris of the S/C and that of the asteroid.

The second optical navigation method is landmark-based OpNav; a technique that becomes possible as Bennu becomes better characterized and a three-dimensional shape model is developed. Landmark OpNav uses defined features on the body’s surface to solve for both the body and S/C positions in the presence of pointing knowledge errors. In situations where the pointing knowledge uncertainties are large, a camera with a large field of view (FOV) is required to capture enough spread between the landmarks to break the degeneracy between pointing and positioning errors. Landmark OpNav for OSIRIS-REx utilizes software called SPC. SPC was developed by Dr. Robert Gaskell with heritage from the Dawn mission and was used as a verification tool for Hayabusa and other small body missions [Gaskell, 2012]. SPC will be used in a limited capacity during Orbital-A to allow for transition from star-based OpNav to landmark OpNav. Landmark-based OpNav will be the primary optical observables used during Detailed Survey through TAG.

Table 2: Camera Specifications

	PolyCam	MapCam	SamCam	NavCam
FOV (deg)	0.8	4	21	33x44
# pixels	1024x1024	1024x1024	1024x1024	2592x1944
Focal Length (mm)	625	125	24	7.6
F-number	3.125	3.4	5.6	3.5
Aperture (cm)	20	3.78	0.428	0.22
microrad/px	13.6	68	354.17	289.5
Pixel Size (microns)	8.5x8.5	8.5x8.5	8.5x8.5	2.2x2.2

Table 2 lists the OSIRIS-REx science Camera Suite (OCAMS) (PolyCam, MapCam and SamCam) and Navigation Camera (NavCam) specifications. Throughout the mission, the primary OpNav imager is the NavCam; how-

ever, there are periods during which the range to Bennu is great enough that long-range imaging must take place with narrower field of view cameras. PolyCam and MapCam will be used for these transitional periods until ranges are close enough for the wide FOV NavCam. Table 3 describes the range criteria for imager usage through the mission.

Table 3: Guideline for imager usage for OpNav imaging technique

Range (km)	Instrument	Technique
> 165	PolyCam	Star-based
30 – 165	MapCam	Star-based
< 30	NavCam	Star-based
33 – 165	PolyCam	Landmark (75 cm)
7.6 – 33	MapCam	Landmark (75 cm)
< 7.6	NavCam	Landmark (75 cm)

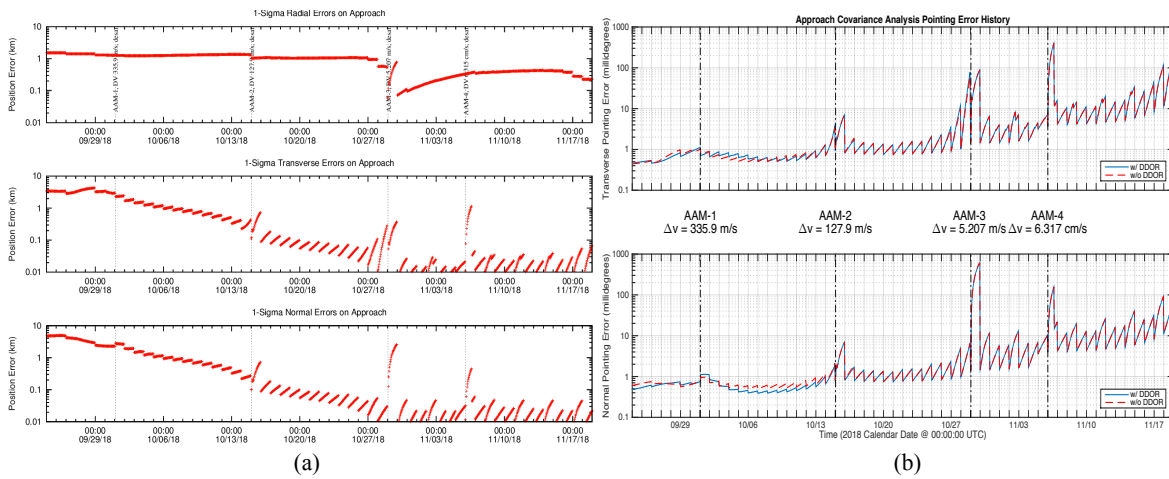
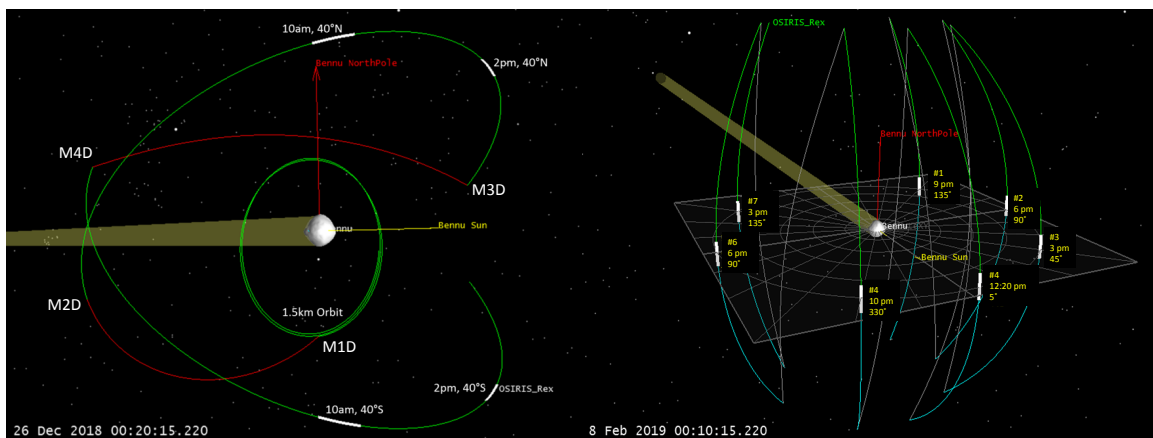


Figure 5: S/C current state errors (1σ) (a) presented in the Radial-Transverse-Normal components relative to Bennu and corresponding trajectory pointing errors (b) during final approach phase

Figure 5 (a) shows the S/C current state Radial-Transverse-Normal (RTN) uncertainties relative to Bennu during Approach. Each point in these plots includes all tracking data up to that point to determine the state. The daily OpNavs are shown in this figure to bring the state errors down substantially; however, the non-gravitational, desat or maneuver errors continue to disperse S/C's state. The small non-gravitation errors are shown to have a more pronounced effect on the state errors as the S/C's position becomes known to the tens to hundreds of meters range. Corresponding pointing errors relative to Bennu in the Transverse and Normal directions are shown in Figure 5 (b).

Detailed Survey

This science sub-phase begins with a maneuver that puts the S/C on a 3.5 km closest approach hyperbolic flyby to allow for imaging of the Northern hemisphere of Bennu. This is followed by another 3.5 km closest approach hyperbolic flyby that targets the Southern hemisphere of Bennu. Both of these flybys target specific solar phase angle stations of Bennu at ± 40 degrees latitude. Figure 6 (a) shows the trajectory and solar phase angle stations of Bennu for this mission phase.



(a) Mid-Latitude Survey

(b) Equatorial Survey

Figure 6: OSIRIS-REx baseline trajectory for Detailed Survey

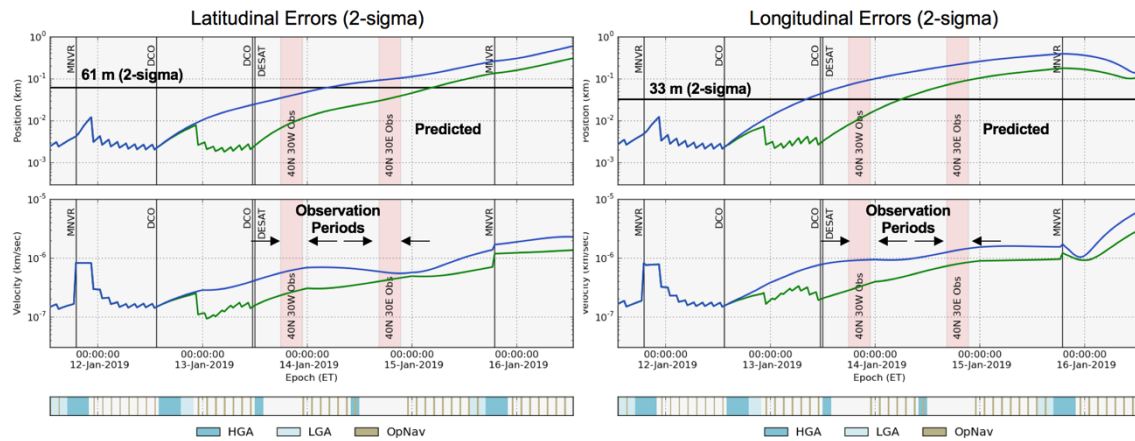


Figure 7: Mid-latitude survey predicted uncertainties for Latitude (left) and Longitude (right) of the first (blue) and second (green) survey stations

During this mid-latitude survey, the S/C’s position must be known to 61 m (2σ) in latitude and 33 m (2σ) in longitude. This phase of Detailed Survey has regular HGA and Low Gain Antenna (LGA) contacts with the DSN, as well as landmark-based OpNav campaigns between DSN passes. The tracking schedule around the observations can be seen in Figure 7. Due to planning and scheduling of the science survey periods, the S/C’s trajectory and uncertainties must be predicted out ~ 30 hours after the data cut-off. Figure 7 shows the predicted latitudinal and longitudinal uncertainties (2σ) predicted over the two survey stations of the Northern Hemisphere. Notice that the longitudinal error requirement is not met for all observations.

With the completion of the mid-latitude survey, an equatorial survey phase begins. This sequence consists of seven equatorial hyperbolic flybys that achieve an altitude of 4.7 km above Bennu’s surface. The S/C will take 4 days to traverse from south to north for each equatorial station with observations being collected for 4.5 hours centered on the equatorial crossing.

Each flyby occurs at different sun illumination conditions in order to map the global texture, geological features, mineralogy, and chemistry of Bennu. Figure 6 (b) shows the trajectory for and equatorial stations for this portion of Detailed Survey. During this sub-phase, regular HGA and LGA contacts with the DSN are made, as well as landmark-based OpNav campaigns between

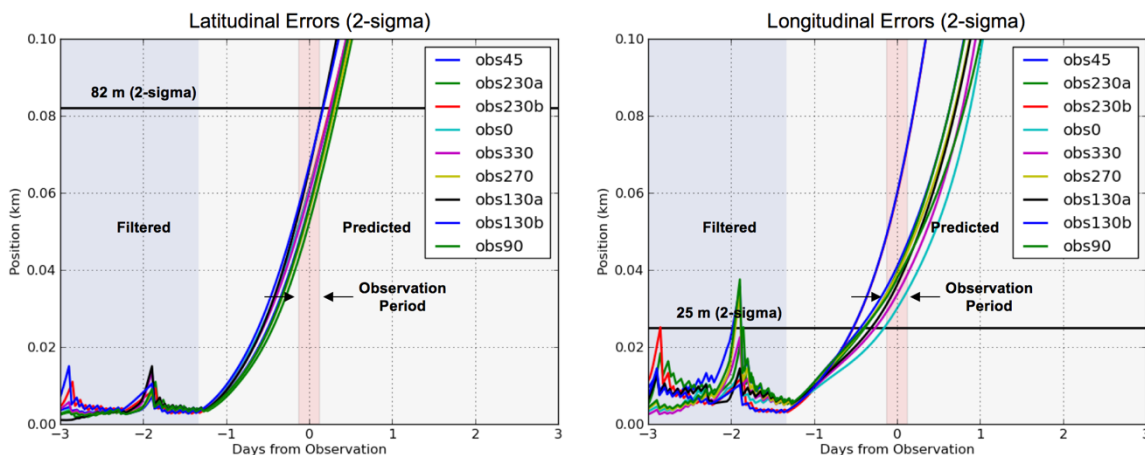


Figure 8: Equatorial survey predicted uncertainties for Latitude (left) and Longitude (right) of all survey stations

DSN passes. Similar to the mid-latitude survey phase, the S/C's trajectory and associated uncertainties must be predicted out ~30 hours prior to the survey. In addition, a desat is performed ~5 hours prior to the start of the survey period. The size of this desat greatly influences the latitudinal and longitudinal predicted uncertainties. Figure 8 shows the predicted latitudinal and longitudinal uncertainties (2σ) predicted over all seven-survey stations relative to the observation period. The predicted uncertainties are consistent for all survey stations. Several iterations with the LM Guidance, Navigation, and Control team were conducted to determine the current best estimate of desat delta-V expected to be imparted on the S/C during this timeframe. The results shown take into account these updated desat performance levels. As with the Mid-latitude survey, the longitudinal requirement cannot be met with the current assumptions for all observations. Discussions are currently underway with the Science Team to determine a resolution since optimistic filter assumptions cannot meet these longitude requirements. The current assumptions for these equatorial observations can meet 2- σ accuracies better than 50 m whereas the Mid-latitude survey can meet accuracies below 100 m.



Figure 9: OSIRIS-REx baseline trajectory for Orbital-B insertion (left) and science (right)

Orbital-B

The completion of Detailed Survey leads into the reestablishment of a stable orbit around Benu known as Orbital-B as shown in Figure 9. The goal of this science sub-phase is to gather global science data and to map in detail twelve candidate sample sites. The duration of this phase is roughly 60 days. The orbit insertion sequence which takes place over 1 week is similar to that of Orbital-A; first a 2-km orbit is established using a set of 3 maneuvers (target insertion to terminator orbit, capture into orbit, then cleanup/trim to 2 km), then the 1-km orbit is achieved with another set of 2 maneuvers. This will be a challenging period for the Navigation Team as the maneuvers are separated by roughly 48 hours. Following a successful stable orbit insertion, nine days of quiescent time is dedicated for Radio Science to acquire minimally perturbed observations for gravity field recovery. This is accomplished by allowing the S/C's trajectory to naturally evolve without any maneuvers during the data arc. During this timeframe, the S/C is in a Sun-pointed attitude. OpNav imaging is acquired when Benu is visible in this attitude configuration. Orbit Laser Altimeter ranging to the asteroid surface is also acquired during this science sub-phase providing detailed measurements of the global shape and topography.

A covariance analysis was performed for the week leading up to the TAG event in mid-October 2019 to determine the state errors at the time of ODM assuming a DCO 24 hours beforehand; these errors are then used to perturb the ODM epoch state in the Monte Carol TAG analysis performed by Berry [2015]. The baseline RTN state errors predicted 1 day after the DCO are presented in Table 4 assuming the nominal Benu GM ($5.2 \text{ m}^3/\text{s}^2$). The challenge for performing the

TAG event is to determine the S/C state given the available optical and radiometric data and accurately predict the state relative to Bennu at the time of the ODM one day later. A requirement is levied on Flight Dynamics that 24-hour predictions of the S/C state shall have in-track position errors less than $85 \text{ m } 3\sigma$; the current 3σ baseline down-track state error is less than 58 m. Note this error is slightly larger than that presented by Berry [2015] of 53 m, where the OD filter did not include OpNav pointing errors. In order to determine the pre-ODM S/C state within the requirements, all the forces affecting the S/C's motion must be well calibrated. Of particular importance is the calibration of small non-gravitational forces ($< 100 \text{ nm/s}^2$) such as SRP, Bennu albedo and Infrared radiation pressure, and the force imparted from the S/C's thermal energy imbalance. Activities that would disturb the orbit such as desats and science observation slews are reduced or eliminated during this time. This orbit is referred to as the safe-home orbit. Two filter strategies were evaluated for the Orbital-B safe-home orbit. These include a baseline case and current-best-estimate (CBE) case. Both cases assumed *a priori* gravity coefficient uncertainties based on the analog of Kaula's rule for Bennu, [McMahon, 2015]. The baseline case assumed that the NavCam pointing can be determined to at least the current best estimate of the S/C (S/C CBE) pointing performance of 1.15 mrad (1σ) with respect to the boresight direction and 1.01 mrad (1σ) in roll about the boresight. The CBE case assumed the SPC process would resolve the image pointing error within the $1-\sigma$ SPC-post-fit pointing errors of 0.42 mrad and 0.40 mrad, respectively with respect to the boresight and roll axes. These errors were set as the process noise to a white-noise-stochastic model with no time correlation between direction and opnav images. The CBE filter case also assumed improved determination of the along-track and radial components of the non-gravitation stochastic acceleration to 1 nm/s^2 , better 2-way Doppler performance and more available landmarks in each image. Appendix A lists the parameter settings for the baseline and CBE filter strategies.

Table 2: Predicted $1-\sigma$ RTN State errors in Orbital-B

Case	Desats in predict	Map Time	R (km)	T (km)	N (km)	DR (km/s)	DT (km/s)	DN (km/s)	Downtrack Timing Error†	Downtrack Pt Error (deg)†	Crosstrack Pt Error (deg)
At DCO											
Baseline	None	10-Oct-19 12:00	0.00077	0.00050	0.00059	6.67E-08	3.27E-08	8.38E-09	.1 min	0.0	0.0
CBE	None	10-Oct-19 12:00	0.00037	0.00026	0.00018	3.31E-08	1.39E-08	4.87E-09	.1 min	0.0	0.0
Baseline	Desats	10-Oct-19 12:00	0.00064	0.00055	0.00038	5.84E-08	9.33E-08	3.90E-08	.1 min	0.0	0.0
CBE	Desats	10-Oct-19 12:00	0.00046	0.00029	0.00031	3.50E-08	7.67E-08	3.13E-08	.1 min	0.0	0.0
Predict 1 day											
Baseline	None	11-Oct-19 12:00	0.00422	0.01915	0.00128	1.42E-06	1.72E-07	1.26E-08	4.4 min	1.1	0.1
CBE	None	11-Oct-19 12:00	0.00156	0.00848	0.00126	6.23E-07	6.19E-08	6.93E-09	2. min	0.5	0.1
Baseline	Desats	11-Oct-19 12:00	0.00714	0.06534	0.00192	4.50E-06	2.40E-07	1.91E-08	15.1 min	3.7	0.1
CBE	Desats	11-Oct-19 12:00	0.00397	0.04358	0.00365	2.92E-06	1.27E-07	1.50E-08	10.1 min	2.5	0.2
Predict 2 days											
Baseline	None	12-Oct-19 12:00	0.00827	0.07797	0.00129	5.64E-06	3.11E-07	3.58E-08	18. min	4.5	0.1
CBE	None	12-Oct-19 12:00	0.00284	0.02849	0.00127	2.06E-06	1.07E-07	1.42E-08	6.6 min	1.6	0.1
Baseline	Desats	12-Oct-19 12:00	0.00987	0.15630	0.00177	1.10E-05	3.40E-07	4.79E-08	36.1 min	9.0	0.1
CBE	Desats	12-Oct-19 12:00	0.00443	0.09716	0.00350	6.65E-06	1.40E-07	2.63E-08	22.5 min	5.6	0.2
Predict 4 days											
Baseline	None	14-Oct-19 12:00	0.01246	0.26360	0.00128	1.90E-05	4.76E-07	1.17E-07	60.9 min	15.1	0.1
CBE	None	14-Oct-19 12:00	0.00421	0.09100	0.00127	6.57E-06	1.60E-07	4.06E-08	21. min	5.2	0.1
Baseline	Desats	14-Oct-19 12:00	0.01659	0.46600	0.00652	3.27E-05	6.76E-07	3.32E-07	107.7 min	26.7	0.4
CBE	Desats	14-Oct-19 12:00	0.01114	0.33810	0.00688	2.33E-05	5.03E-07	3.01E-07	78.1 min	19.4	0.4
Predict 1 week											
Baseline	None	17-Oct-19 12:00	0.01299	0.65639	0.00126	4.74E-05	7.01E-07	2.97E-07	2.53 hr	37.6	0.1
CBE	None	17-Oct-19 12:00	0.00431	0.22273	0.00123	1.61E-05	2.34E-07	1.00E-07	.86 hr	12.8	0.1
Baseline	Desats	17-Oct-19 12:00	0.01544	1.08200	0.00799	7.71E-05	1.04E-06	8.32E-07	4.17 hr	62.0	0.5
CBE	Desats	17-Oct-19 12:00	0.00970	0.81300	0.00750	5.75E-05	8.27E-07	7.52E-07	3.13 hr	46.6	0.4
Predict 2 weeks											
Baseline	None	24-Oct-19 12:00	0.05982	1.98251	0.00298	1.47E-04	9.73E-07	9.27E-07	7.64 hr	113.6	0.2
CBE	None	24-Oct-19 12:00	0.02007	0.66615	0.00133	4.93E-05	3.36E-07	3.10E-07	2.57 hr	38.2	0.1
Baseline	Desats	24-Oct-19 12:00	0.09809	2.97300	0.01878	2.19E-04	1.66E-06	1.78E-06	11.45 hr	170.3	1.1
CBE	Desats	24-Oct-19 12:00	0.07545	2.20400	0.01841	1.62E-04	1.74E-06	1.45E-06	8.49 hr	126.3	1.1
Predict 4 weeks											
Baseline	None	7-Nov-19 12:00	0.33541	6.77591	0.01586	6.01E-04	1.37E-06	3.85E-06	26.1 hr	388.2	0.9
CBE	None	7-Nov-19 12:00	0.11252	2.26719	0.00296	2.01E-04	6.43E-07	1.45E-06	8.73 hr	129.9	0.2
Baseline	Desats	7-Nov-19 12:00	0.50120	8.98400	0.04247	8.04E-04	4.05E-06	6.05E-06	34.61 hr	514.7	2.4
CBE	Desats	7-Nov-19 12:00	0.34060	6.10400	0.04374	5.46E-04	5.39E-06	6.73E-06	23.51 hr	349.7	2.5

* Desats are approx. 3-4 days begin on 10/8/19 12:00, 10/12/19 12:00, 10/15/19 12:00, 10/18/19 12:00, 10/21/19 12:00, 10/24/19 12:00

† Assumes circular orbit for mapping transverse error directly into timing and downtrack pointing errors

The epoch of the data arc begins October 6, 2019. The date of the ODM which places the S/C along the TAG trajectory was October 11, 2019 at 12:00 UTC and the DCO for this maneuver is 24 hours beforehand (Oct 10, 2019 12:00 UTC). Daily HGA telecom passes are assumed, where the S/C will slew to point the HGA towards Earth while keeping the Sun within the S/C's X-Z plane. In the safe-home orbit, these Earth contacts will be limited to 5 hours or less to ensure as stable thermal conditions as possible. This

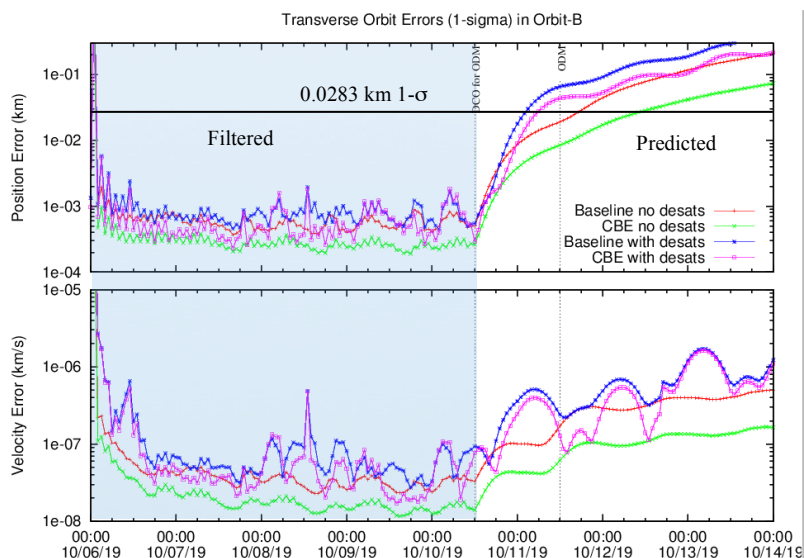


Figure 10: Comparing the 1- σ filtered and predicted transverse state errors

covariance analysis also evaluated the growth in the state errors in Table 4 from 1 day to 4 weeks after the DCO for both the baseline and CBE filter strategies assuming either no desat errors or with desats (ΔV errors of 0.5 mm/s) every 3 days over the predicted time. Since the transverse errors at the map time of 4 days or greater in the linear covariance analysis can be larger than the orbit radius, it is assumed that these errors map directly into orbit down-track timing or true anomaly errors in the 1-km circular orbit. Thus, it will be a challenge to plan specific science observations 4 weeks ahead, since the predicted transverse errors approach the circumference of the 1-km orbit of 6.3 km, which corresponds to a true anomaly error of 360° , i.e. the S/C's location in orbit is unknown after 4 weeks. The adopted strategy for targeting specific science observations requires late OD updates similar to ODM with DCO of 24-30 hours from the start of the observations. The CBE no-desat case improves the state errors by a factor of 2–3 of the baseline. Desat errors nearly double the baseline or triple the CBE no-desat case predicted transverse errors. Figure 10 compares the 1- σ transverse position and velocity filtered and predicted errors for the baseline and CBE filter cases. The baseline-filtered cases generally show position errors less than 1 m, while the CBE no-desat state errors are less than 50 cm. The reconstructed velocity errors for all cases are generally less than 0.1 mm/s.

CONCLUSIONS

The mission plan for the OSIRIS-REx mission will require unprecedented levels of navigation performance, and will require the Operations teams to execute a rapid cadence of maneuvers and observation plans. This mission requires the OD-predicted S/C state errors during proximity operations with Bennu to be on the order of tens of meters. Requirements at these levels are a challenge to meet, especially since these are at least 1–2 orders of magnitude lower than previous planetary or small body missions. It will also be challenging to meet the demanding ProxOps operations schedule, which requires frequent OD updates for maneuver designs or late science updates. Furthermore, at close range to Bennu, the on-board ephemeris needs frequent updates from the OD Team (at least twice per week) to ensure the asteroid remains within the FOV of the NavCam. It has been shown that the Detailed Survey longitudinal requirements are not yet met, even with CBE levels of non-gravitational forces or improved desat performance. The Navigation

Team is in discussions with the Science Team to better understand the impact of relaxing these requirements on the science observations planned during each Detailed Survey pass. The primary challenge during the Orbital-B phase is to characterize the non-gravitational forces at or below the 3 nm/s^2 level. Given that we can determine the non-gravitational errors to this level, the state errors predicted 24 hours after the DCO for the ODM have been shown to be within the requirements, which ensures a successful TAG attempt.

ACKNOWLEDGMENTS

This work is supported by the OSIRIS-REx Asteroid Sample Return Mission managed for NASA by the Goddard Space Flight Center in Greenbelt, MD. The Principal Investigator is Dr. Dante Lauretta of the University of Arizona in Tucson. Lockheed Martin Space Systems in Denver is building the spacecraft. The authors wish to thank Christian May and Miranda Stoll of LM for the spacecraft thermal models.

REFERENCES

- Berry, K., P. Antreasian, M. Moreau, A. May, B. Sutter, "OSIRIS-REx Touch-And-Go (TAG) Navigation Performance," AAS-15-125, AAS GNC Conference, Breckenridge, CO, Jan 30–Feb 4, 2015.
- Sugimoto, Y. and Jozef C. van der Ha, "Thermal Radiation Model for the Rosetta Spacecraft," In AIAA/AAS Astrodynamics Specialist Conference, Toronto, Ontario Canada, AIAA 2010-7659, Aug 2-5 2010.
- Shoemaker, M., Jozef C. van der Ha, and Trevor Morley, "Modeling and Validation of Thermal Radiation Acceleration on Interplanetary Spacecraft," *Journal of Spacecraft and Rockets*, 49(2), March-April 2012.
- Antreasian, P.G. and G.W. Rosborough, "Prediction of Radiant Energy Forces on the TOPEX/Poseidon Spacecraft," *Journal of Spacecraft and Rockets*, 29(1):81–90, Jan-Feb 1992.
- Vigue, Y., B. Schutz, and P. Abusali, "Thermal Imbalance Force Modeling for GPS Satellites Using the Finite Element Method," *Journal of Spacecraft and Rockets*, 31(5), September-October 1994.
- Fahnestock, E.G., Ryan S. Park, Dah-Ning Yuan, and Alex S. Konopliv, "Spacecraft Thermal And Optical Modeling Impacts on Estimation Of The GRAIL Lunar Gravity Field," In AIAA/AAS Astrodynamics Specialist Conference, Minneapolis, Minnesota, Paper AIAA 12-3077, August 13-16 2012.
- Olds, R., "Surface Property Data for Solar Radiation Pressure Modeling," GNC Technical Memo NFP3-AC-13-0022, Lockheed-Martin Co, October 2013.
- Jackman, C.D., D.S. Nelson, P.J. Dumont, W.M. Owen, M.W. Buie, S.A. Stern, H.A. Weaver, L.A. Young, K. Ennico, C.B. Olkin, "New Horizons Optical Navigation on Approach to Pluto," AAS-16-083, AAS GNC Conference, Breckenridge, CO, Feb 5-10, 2016.
- Gaskell, R.W., "SPC Shape and Topography of Vesta from DAWN Imaging Data", AAS/Division for Planetary Sciences Meeting Abstracts, 2012, 44, Oct, 209.03.
- McMahon, J.W., D.J. Scheeres, D. Farnocchia, S.R. Chesley, "Optimizing Small Body Gravity Field Estimation Over Short Arcs," Paper AAS-15-669, AAS Astrodynamics Specialist Conference, Vail, CO, Aug. 9-13, 2014.

APPENDIX A: FILTER STRATEGY

Error Source	Estimate, Consider or Observable	A Priori Uncertainty (1 σ)	Correlation Time	Update Time or Frequency	Comments
Tracking Data					
X-Band 2-way Doppler (mm/s)	Obs	Baseline: 0.1 CBE: 0.073	-	-	0.1 mm/s = 0.0055 Hz, data deweighted for solar conj. (sep < 10 deg)
X-Band Range (m)	Obs	3.333	-	-	23.3 RU (1 m = 7.0 RU), data deweighted for solar conj. (sep < 10 deg)
OPNAV (Landmarks) Line/Pixel (pix)	Obs	$W = (W_{min}^2 + (S/R)^2)^{1/2}$ Orbit-B Safe-home 3.3-3.6	-	-	$W_{min} = 1$ pix, $S = 75$ cm (shape model error), $R =$ camera resolution
Spacecraft Trajectory Models					
Epoch state position (km)	Estimate	5000	-	-	Earth, Sun or Bennu-Centered ICRF Cartesian
Epoch state velocity (km/s)	Estimate	0.5	-	-	
Solar Radiation Pressure Coefficient (% of total)	Estimate	20	-	-	GR (or SOLCOF)
Non-Grav Acceleration (km/s ²)	Estimate	Baseline: 3.00E-12 per axis CBE: 3e-12 in sun dir, 1e-12 radial, transverse	0	1 day	Baseline: assumes 8% SRP in all axes CBE: assumes calibration of transverse and radial components
AMD Event ΔV (mm/s)	Estimate	2 mm/s for 10-day freq. 0.5 mm/s for 3-day freq. CBE used in DS: < 0.1 mm/s	-	-	Per axis, Impulsive ΔV
Data biases and other info					
Range Bias (m)	Estimate	4	0	Per pass	RSS of DSN and S/C errors
Number of landmarks (in view of opnav)		Baseline: 7-10 CBE: 17-21	-	-	Total landmarks in simulation: Baseline:40 CBE: 100
Camera Pointing (deg)	Estimate	Baseline: S/C's CBE(1sig): 1.1 mrad boresight 1.01 mrad roll CBE: Post-SPC(1sig): 0.42 mrad boresight 0.47 mrad roll	-	Per OpNav image	Assume Rayleigh distribution for per axis errors (3-sig boresight error/3.439), Scale RA error by 1/cos(dec)
Ephemerides					
Earth/Moon Barycenter Ephemeris	Consider	JPL DE425 Covariance	-	-	Set III parameters
Bennu Ephemeris					
Epoch state position (km)	Estimate	JPL Soln #76 correlated covariance	-	-	Set III parameters (1 X formal statistics). Formal position error on approach ~10 km.
Epoch state velocity (km/s)	Estimate		-	-	
Gravity					
Earth GM (kg ³ /km ²)	Consider	1.40E-03	-	-	
Lunar GM (kg ³ /km ²)	Consider	-	-	-	
Bennu GM (kg ³ /km ²)	Estimate	100% of nominal GM on approach & Prelim. Survey, 10% afterwards (5.2e-9 - 5.2e-10)	-	-	Nominal GM = 5.2 e-9 kg3/km2
Earth Gravity Field	Consider	-	-	-	Correlated covariance from JGM-3
Lunar Gravity Field	Consider	-	-	-	Correlated covariance from LP150Q
Bennu Gravity Field	Estimate	4x4, Kaula power law based on Bennu	-	-	Based on current range of errors in shape model. [McMahon, 2015]
Measurement Models					
Station Locations (km, deg, km)	Consider	JPL 2003 full correlated Covariance	-	-	Stations 15, 45, 65 used in cov studies (2-5 cm each axis)
Earth Pole X, Y (cm)	Consider	10.0 / 10.0	-	-	15 nanoradians
UT1 (cm)	Consider	10	-	-	0.256 msec
Ionosphere – day / night (cm)	Consider	55.0 / 15.0	-	-	S-band values (MIRAGE input) eqv to 15, 4 cm for X-band
Troposphere – wet / dry (cm)	Consider	1.0 / 1.0	-	-	
Bennu Orientation Model (Principal axis rotation)					
Pole RA, Dec (deg)	Estimate	10, 10	-	-	
Prime Meridian (deg)	Estimate	100	-	-	
Spin (deg/s)	Estimate	1.20E-03	-	-	100 deg/day